Meteorology and Atmospheric Physics (2023) 135:10
https://doi.org/10.1007/s00703-022-00946-x

ORIGINAL PAPER

One-hour-ahead solar radiation forecasting by MLP, LSTM, and ANFIS approaches

Alper Yildirim[1] · Mehmet Bilgili[2] · Arif Ozbek[2]

Received: 21 May 2022 / Accepted: 6 December 2022 / Published online: 16 December 2022
© The Author(s), under exclusive licence to Springer-Verlag GmbH Austria, part of Springer Nature 2022

Abstract
The use and importance of renewable energy sources (RES) have been increasing every passing year as fossil fuels will soon be depleted. Within this context, solar-photovoltaic (PV) is the most preferred energy type among RES. The PV has uncertain power output as its output depends on solar radiation, which is heavily influenced by environmental factors, so the prediction of solar radiation plays a crucial role in integrating these plants into the electricity grid. For the short-term 1-h-ahead solar radiation prediction, four time-series methods were implemented in this study: long short-term memory (LSTM) network, multilayer perceptron (MLP), and adaptive neuro-fuzzy inference system (ANFIS) with grid partition (GP), and fuzzy c-means (FCM). Root mean square error (RMSE), correlation coefficient (R), and mean absolute error (MAE) were used as statistical error criteria. The obtained results by the LSTM, MLP, ANFIS-FCM and ANFIS-GP models were assessed by comparing with the actual data. Considering the testing procedure, the best MAE values were found to be 53.37 W/m^2, 58.45 W/m^2, 61.68 W/m^2, and 78.17 W/m^2 for the LSTM, ANFIS-FCM, MLP, and ANFIS-GP, respectively. Results showed that the LSTM model in 1-h-ahead solar radiation prediction yielded the best results among all four models with high accuracy.

1 Introduction

Since the nineteenth century, industrialization and the human population have been increasing in the world. In parallel with this increase, electricity consumption has also drastically risen (Abdulkarim et al. 2020). Global energy demand will increase by 30% from 2016 to 2040 according to the report (WEO) published in 2017 (Ghimire et al. 2019). World countries have met most of their energy needs from fossil fuels. However, consumption of these fuels causes global warming, pollution of air by poisonous gases into nature, environmental problems such as ozone layer perforation, acid rains (Dinçer 2011). These problems cause great harm to human health and nature. In addition, it is predicted that these resources, which are limited in the world, will end in 2090. For this reason, researchers and commercial organizations have turned to alternative energy sources that are easy to use, abundant in nature, and less polluting the environment, to overcome the commitment to fossil fuels. Accordingly, studies on renewable energy sources (RES) such as solar, wind, biomass, geothermal have been carried out. These sustainable energies are not only renewable, but they also protect ecology and the environment (Pandey and Katiyar 2013).

Solar energy is one of the most plentiful yet underutilized RES that has the potential to provide enormous amounts of electricity (Bilgili and Ozgoren 2011). Throughout the year, the earth's surface gets average solar radiation of 1367 W/m^2, which equates to roughly 1.8×1011 MW. Such an enormous and limitless source of energy is more than enough to meet all of the world's power needs. Solar energy has emerged as a promising source of power generation in recent years, with the potential to replace conventional sources (Kumari and Toshniwal 2021). Solar PV had a record-breaking year in 2020, with an approximate 139 GW added to a total of 760 GW. Solar PV accounts for nearly 60% of all renewable energy capacity worldwide (IRENA 2021).

Responsible Editor: Clemens Simmer, Ph.D.

✉ Alper Yildirim
alperyildirim@osmaniye.edu.tr

[1] Department of Machinery and Metal Technology, Osmaniye Vocational School of Higher Education, Osmaniye Korkut Ata University, 80000 Osmaniye, Turkey

[2] Department of Mechanical Engineering, Ceyhan Engineering Faculty, Cukurova University, 01950 Adana, Turkey

Nevertheless, solar energy sources cannot ensure that electricity is produced continuously over time. Moreover, energy storage technology is insufficiently developed for the storage of electricity when it is required. As a result, the grid operators face a significant challenge in integrating solar energy sources into the electric grid. Grid operators should maintain grid stability indefinitely so that supply matches demand. To meet peak demand and avoid a blackout, grid operators plan ahead of time by mobilizing various sources such as RES and conventional power. Nonetheless, solar radiation fluctuations, primarily caused by clouds, reduce electricity production and make it more difficult for grid operators to maintain a balance between consumption and production (Sharifi et al. 2022).

Predicting PV electricity production significantly assists in overcoming this barrier by facilitating grid management through planning and maintenance. Researchers have developed a variety of methods to achieve this goal (Ali-Ou-Salah et al. 2021). The literature in this field enables us to categorize solar prediction methods into three groups. These are (1) short-term prediction, (2) medium-term prediction, and (3) long-term prediction. Besides, to predict solar radiation correctly four different models are found in the literature. These are (1) physical, (2) empirical (3) machine learning, and (4) statistical models. Physical models, such as sky view-based models, are used to investigate the relationship between SR (solar radiation) and other meteorological parameters. It has a strong physical basis, but the structure of the physical models is complex due to the complex conditions of the atmosphere. One of the most popular models is the empirical model, which is used to develop a linear regression or nonlinear regression equation. Although empirical models are simple and easy to use, their accuracy is usually limited. Based on the statistical correlation, statistical models such as the autoregressive moving-average model (ARMA) and the autoregressive integrated moving-average model (ARIMA) are developed. They are usually more accurate than empirical models, but they cannot adequately describe the nonlinear correlation between SR and other parameters. Machine-learning models, such as artificial neural networks (ANNs) (Ozgoren et al. 2012), support vector machines (SVMs) (Chen and Li 2014), and adaptive neural-fuzzy inference systems (ANFIS) (Mirbolouki et al. 2022) outperform empirical, physical, and statistical models in terms of accuracy and application. They become one of the most popular models ANN (Zhou et al. 2021) models that are commonly used include multilayer perceptron (MLP) (Kim et al. 2019) and radial basis function network (RBFN) (Dhakal et al. 2020). They were able to predict short-term, medium-term, and long-term SR with moderate accuracy (Zhou et al. 2021). The fourth category is hybrid models are used to improve forecasting accuracy by combining two or more methods. Hybrid models benefit from each method, improving the overall model's performance. Many hybrid models combining machine learning (ML) algorithms, physical models, mathematical methods, and optimization algorithms have been proposed in the literature (Akhter et al. 2019). In terms of predicting accuracy, the hybrid models outperform the individual methods. The hybrid models, on the other hand, have high computational complexity, necessitating significant time and space resources to run. Furthermore, their performance is heavily reliant on historical inputs, which must be carefully chosen (Ali-Ou-Salah et al. 2021).

ML models have attracted researchers due to their high prediction accuracy and ease of use. Chen et al. (2019) investigated the transferability of SVM for predicting SR from temperature data and concluded that the SVM could be used to predict SR. Furthermore, they discovered that the distance and diurnal temperature range between two locations affected SVM accuracy. A temperature-based corrected SVM model for SR estimation was presented by Guermoui et al. (2020). This model is created by fusing an SVM model for SR prediction and an SVM model for SR error estimation. This method has improved the performance of SVM. Linares-Rodriguez et al. (2013) used satellite irradiances to predict SR in Spain using the MLP model. The model performs well in both clear and cloudy sky conditions. Sözen et al. (2004) estimated solar radiation in Turkey using an ANN model with geographical and meteorological data as input variables. The MLP network has a MAPE of 6.73%.

Numerous recent studies have used ANFIS with various inputs to predict SR. Piri and Kisi (2015) created an ANFIS model with data from humidity, sunshine, and temperature as inputs. Benmouiza and Cheknane (2019) created several hybrid models based on the ANFIS model and used various clustering algorithms such as grid partitioning, fuzzy c-means (FCM), and subtractive clustering to forecast hourly solar radiation in Algeria. Mohammadi et al. (2016) developed the ANFIS procedure to determine the best input parameters for SR prediction. They concluded that temperature could be a critical input parameter. Naderloo (Naderloo 2020) predicted daily SR using ANN and ANFIS models with meteorological factors such as temperature, relative humidity, and precipitation. In comparison to ANFIS, the ANN model produced slightly better results. Wang et al. (2017) used ANFIS with grid partitioning and ANFIS with subtractive clustering (ANFIS-SC and ANFIS-GP). Pressure, sunlight, humidity, and temperature data were used as inputs in these models. Classical model MLR and various AI methods, including ANFIS, were used to estimate daily global SR in Iraq using various metrological parameters (Nourani et al. 2019). The results demonstrated that the ANFIS method outperforms other predictive models in terms of accuracy. Sthitapragyan et al. (2015) estimated the monthly mean global solar radiation in 3 different regions

in Eastern India with ANFIS, Radial Basis Function (RBF), and Multi-layer Perceptron (MLP) methods. Compared with the meteorological data, the ANFIS method yielded significantly successful results compared to the other two methods. A comparison of different AI models in SR prediction revealed that the ANFIS method is appropriate for SR estimation due to its ability to capture the uncertainty associated with time-series data (Tao et al. 2021).

Deep learning in time-series modeling has piqued the interest of many researchers in recent years. Time-series forecasting systems can predict future behavior by analyzing past and current status information. Deep artificial neural networks with the ability to learn complex and nonlinear relationships in data can manually determine the effective properties of time-series data. One of several models that can accommodate dependencies between consecutive time steps is the recurrent neural networks (RNN) algorithm. Long short-term memory-LSTM is an RNN model that has been modified. Solving the problem of vanishing gradient and the ability to process long time series are the primary advantages of the LSTM model over RNN. Recently, the LSTM model has been used in several time-series forecasting studies, including rainfall forecasting (Zhang et al. 2020), traffic speed prediction (Ma et al. 2015), air quality forecasting (Li et al. 2017), evapotranspiration forecasting (Yin et al. 2020), electricity load forecasting and stream flow forecasting (Chen et al. 2020).

LSTM model has been successfully applied for SR forecasting in recent studies (Mirbolouki et al. 2022). Huynh et al. (2020) used LSTM to predict 1- to 30-min ahead SR using data from Bac Ninh in Vietnam from 2017 to 2019. In comparison to ARIMA, MLP, CNN, and SVM, LSTM gave the highest accuracy with R greater than 0.90. Araujo compared hourly solar radiation data obtained over 3 months using Weather Research and Forecasting (WRF) and LSTM models. Successful forecasting results were obtained with both the models. Although the researcher found that the WRF model has a lower error rate compared to the LSTM algorithm, he suggested that the LSTM model can be used for long-term prediction (de Araujo 2020). Sorkun et al. (2020) applied the LSTM model to multivariate SR data with a 1-h horizon for prediction. The results indicate that the LSTM model is competitive and appropriate for the 1-h time-series prediction of multivariate SR data. Obiora et al. (2020) estimated the hourly SR using the LSTM model in Johannesburg city. The prediction accuracy of the proposed model was compared with the SVR, and the simulation results outperformed the SVR model by 3.2% in the normalized root mean square error (nRMSE) of the proposed LSTM network.

Accurate SR forecasting is critical for ensuring optimal integration of large-scale solar-PV plants with the public electricity grid, planning for the future, and making policy. Moreover, for grid-connected PV technologies, especially in variable atmospheric conditions, accurate estimation of SR is required. Estimating SR is also necessary for ensuring grid programming, grid energy management, and grid operation. This study's main original contributions to the literature can be summarized in four categories:

(1) In this study, LSTM, ANFIS-FCM, ANFIS-GP, and MLP models were performed for forecasting 1-h-ahead SR data.
(2) Since it makes predictions by taking into account the hidden periodicity in the data, the time-series approach based on the LSTM neural network allows for the use of historical data as an independent variable. As a result, when the LSTM neural network model is used for time-series estimation of the SR, more accurate results are obtained when compared to statistical models proposed in the literature, as demonstrated in this study.
(3) The main advantage of the proposed models is that they can accurately predict SR utilizing only solar radiation data. These methods are optimal for estimating solar radiation in fast-changing and fluctuating weather. In addition, these methods are dependent on no geographic or meteorological parameters for precise estimation. This is essential, particularly for developing countries where climatic variables (such as wind speed and relative humidity) missing or are not available due to technical reasons.
(4) First-time applied here, to demonstrate the efficacy of the proposed method, the results of the LSTM model were compared to the findings of the ANFIS-GP, ANFIS-FCM, and MLP models. In addition, the results from this study were compared with those obtained from similar studies published in the literature.

2 Methods

2.1 ANFIS: adaptive neuro-fuzzy inference system

ANFIS, which emerged with the study by Jang in 1993, is expressed as a mixed system that includes Fuzzy Inference Systems (FISs) and ANN (Jang 1993). It integrates the ability of fuzzy logic philosophy to benefit from the human thought system and the learning ability of artificial neural networks. ANFIS is a neurally fuzzy model that can adapt itself to learning. ANFIS learns by defining parameter values to reduce the error between estimated output and actual output. ANFIS algorithm is a hybrid program formed by the combination of the least-squares model and the backpropagation learning algorithm (Çakin 2019).

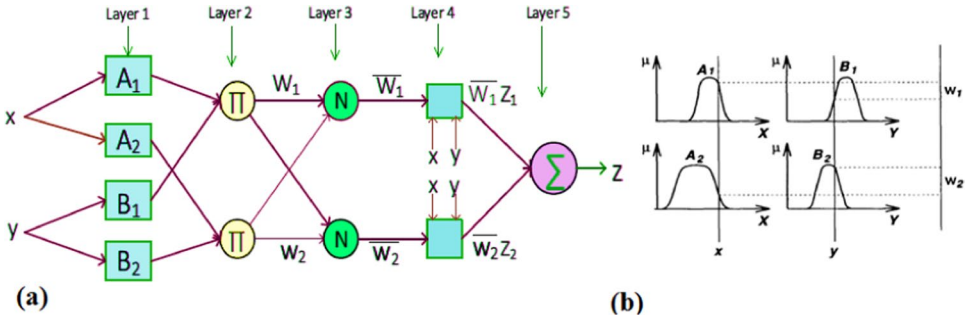

Fig. 1 **a** ANFIS architecture (Adeleke et al. 2022). **b** Sugeno-type fuzzy inference with two inputs and two rules (Şenocak 2018)

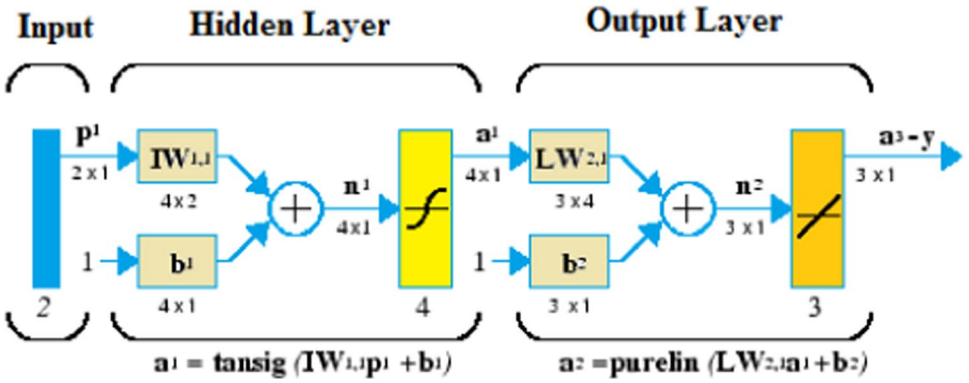

Fig. 2 A single-layer S logsig neuron network with R inputs (Aguinaga et al. 2017)

ANN is used to set and find the rules and variables of the ANFIS system. There are two important steps in ANN systems structural and variable adjustments. The variable setting includes the weights, shapes, and calculation of rule functions of membership functions. In structural adjustment, the number of rules and variables involves blurring each input and output variable and creating rules. ANFIS architecture consisting of two inputs (x and y), single-output (f), and 4 rules are given in Fig. 1 (Turan 2018).The ANFIS structure is a network structure capable of neural learning that represents Sugeno fuzzy systems. This network is made up of nodes that are organized into layers to perform specific functions. The fuzzy "if–then" rules for a two-input, one-output system as x and y can be written as follows (Azizi and Izadfar 2019):

$$Rule\ 1: if\ x\ is\ A_1\ and\ y\ is\ B_1,\ then\ z_1 = p_1x + q_1y + r_1 \tag{1}$$

$$Rule\ 2: if\ x\ is\ A_2\ and\ y\ is\ B_2,\ then\ z_2 = p_2x + q_2y + r_2 \tag{2}$$

where A_i and B_i represent the fuzzy clusters in the leader and p_i, q_i, and r_i represent the design parameters in the training process. Circles and squares can be used to reflect adaptive capabilities. The square shows the adaptive node, while the circle shows the fixed node. The parameter can be changed during adaptation or training. ANFIS consists of neural network and fuzzy logic integration (Şenocak 2018). The real output of the network is given as follows:

$$f = \frac{w_1f_1 + w_2f_2}{w_1 + w_2} \Rightarrow f = \overline{w}_1f_1 + \overline{w}_2f_2 \tag{3}$$

ANFIS has five layers. This system is depicted in Fig. 1. The node functions of each layer in the ANFIS structure, as well as the operation of the layers, are as follows:

Layer 1: This layer is being used to specify an input variable for each of the relevant fuzzy sets. The nodes in this layer show how membership degrees are generated using membership functions. A node i's node function is defined as follows:

$$O_i^1 = \mu_{A_i}(x), \quad i = 1, 2 \tag{4}$$

$$O_i^1 = \mu_{B_{i-2}}(y), \quad i = 3, 4 \tag{5}$$

where μ_{A_i} and μ_{B_i} are the MFs. The parameters in this layer are called preliminary parameters.

Layer 2: In this layer's nodes, incoming signals are copied and the output is sent. Each node in this layer multiplies to determine the firing strength of a rule.

$$O_i^2 = w_i = \mu_{A_i}(x)\mu_{B_i}(y), \quad i = 1, 2 \tag{6}$$

Layer 3: This layer's ith node computes the ratio of the ith rule's firing strength to the sum of all rules' firing strengths:

$$Q_i^3 = \overline{w}_i = \frac{w_i}{w_1 + w_2}, \quad i = 1, 2 \tag{7}$$

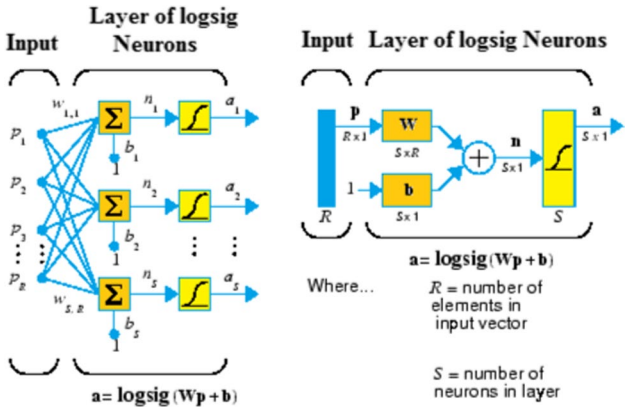

Fig. 3 The two-layer tansig/purelin feed-forward neural network's appropriate notation (Aguinaga et al. 2017)

where $\overline{w}_i$ is called the normalized firing strengths.

Layer 4: In this layer, node I use the node function shown below to calculate the effect of the *i*th rule on model output:

$$Q_i^4 = \overline{w}_i z_i = \overline{w}_i \left(p_i x + q_i y + r_i\right), \quad i = 1, 2 \tag{8}$$

$\overline{w}_i$ and $\{q_i, p_i, r_i\}$ denotes the layer 3 output and the parameter set, respectively. The consequences' parameters are the parameters in this layer.

Layer 5: This layer is referred to as the output nodes, with a single node calculating the overall output as the sum of the all the incoming signals expressed as (Park et al. 2019)

$$Q_i^5 = \sum_{i=1}^{2} \overline{w}_i z_i = \frac{w_1 z_1 + w_2 z_2}{w_1 + w_2} \tag{9}$$

Data structures in cluster analysis can be divided into groups or clusters, which is a significant task in machine learning and data mining algorithms. Data points in the same group are similar but not identical to data points in other groups. Clustering is a critical step in constructing an ANFIS structure because it is necessary to group data points into similar fuzzy clusters and assign and generate a fuzzy inference system structure and membership functions (MF) for the data. Furthermore, in ANFIS modeling, clustering defines the form of fuzzy rules and optimal numbers. This is accomplished through the use of common clustering algorithms including grid partitioning, fuzzy c-means, and subtractive clustering. Because of the noticeable impact of clustering techniques on the ANFIS model's achievement in approximating an output function, it must be carefully chosen within the ANFIS model structure. ANFIS-GP and ANFIS-FCM are two common ANFIS clustering techniques (Adeleke et al. 2022).

2.1.1 Fuzzy c-means clustering

The fuzzy c-means (FCM) algorithm is a purpose function-based model, and it is based on the principle that the data can be assigned to more than one cluster with varying degrees of membership. Following Dunn's introduction of this algorithm in 1973 (Dunn 1973), Bezdek (2003) developed it in 1981. FCM divides a set of n vectors $x_i = 1, 2\ldots, n$ into fuzzy groups and finds a cluster center for each group by lowering the objective function of the dissimilarity measure. $i = 1, 2,\ldots,$ c is randomly chosen from the n points. FCM method consists of 4 steps (Abdulshahed et al. 2015): the centers of each cluster $c_i = 1, 2,\ldots,$ c are randomly selected from the n data patterns $\{x_1, x_2, x_3,\ldots, x_n\}$ in the first step. The membership matrix (μ) is computed in the second step using the following equation:

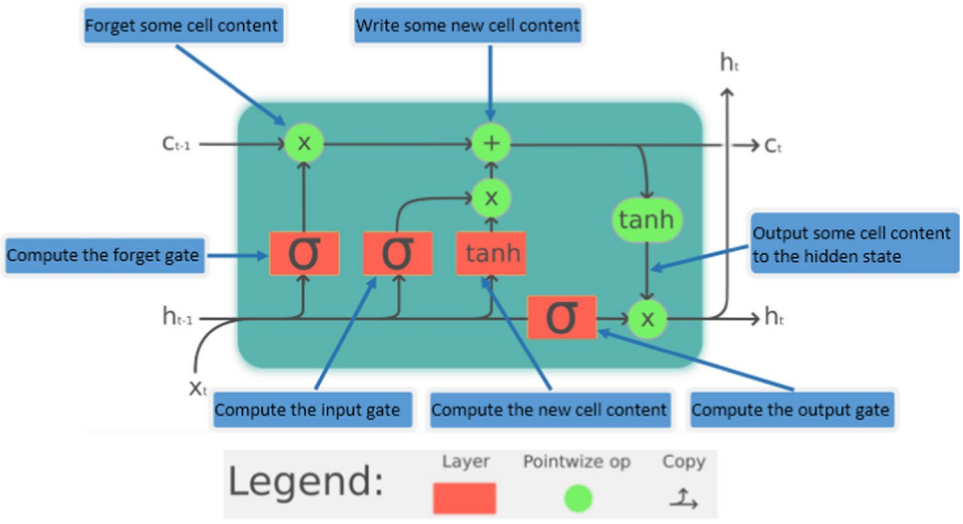

Fig. 4 LSTM architectural structure (Xiao and Yin 2019; Liu et al. 2021)

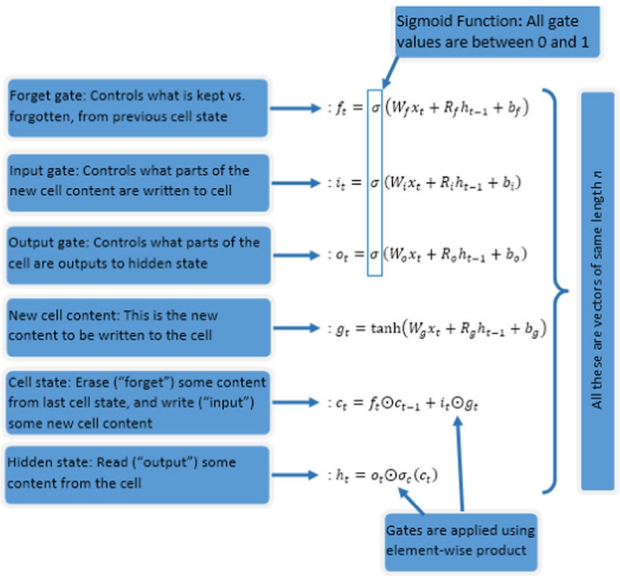

Fig. 5 LSTM unit mathematical formulas and explanations (Qing and Niu 2018)

$$\mu_{ij} = \frac{1}{\sum_{k=1}^{c} \left(\frac{d_{ij}}{d_{kj}}\right)^{\frac{2}{m}-1}} \tag{10}$$

where μ_{ij} is the degree of membership of object j in cluster i; m is the degree of fuzziness (m > 1); $d_{ij} = ||c_i x_i||$: x_i and c_i's Euclidean distance.

The objective factor is determined in the third step using the following equation:

$$J(U, c_1, c_2 \ldots .c_c) = \sum_{i=1}^{j} j_i = \sum_{i=1}^{c} \cdot \sum_{j=1}^{n} \mu_{ij}^{m} d_{ij}^{2}. \tag{11}$$

If the process falls below a certain threshold, it is halted. The new c fuzzy cluster centers $c_i = 1, 2, \ldots$, c is calculated in the final step using the following equation:

$$c_i = \frac{\sum_{j=1}^{n} \mu_{ij}^{m} x_j}{\sum_{j=1}^{n} \mu_{ij}^{m}} \tag{12}$$

2.1.2 Grid partitioning (GP)

The fuzzy partitioning techniques include tree partitioning, grid partitioning, and scatter partitioning. The input space is partitioned into rectangular subspaces using axis parallel partitioning based on the type and number of the pre-defined membership function in this method. Because of the exponential relationship between the number of input n and the number of fuzzy rules m, which results in a fuzzy rule number of nm and a large memory size requirement, the use of a small number of membership functions is required (Kim et al. 2019). Further information regarding this technique can be obtained from Abonyi et al. (1999).

2.2 Multi-layer perceptron (MLP)

Static neural networks and dynamic neural networks are two types of neural networks. MLP is one of the most widely used static networks (Moghaddamnia et al. 2009), in which the input and desired output are presented to the network, and the weights are adjusted so that the network tries to produce the desired output. A hidden, an input, and an output layer are the three layers of neurons (nodes) in the MLP network. Each layer's neurons are the fundamental elements, and each neuron in one layer is associated with and interacts with neurons in other layers.

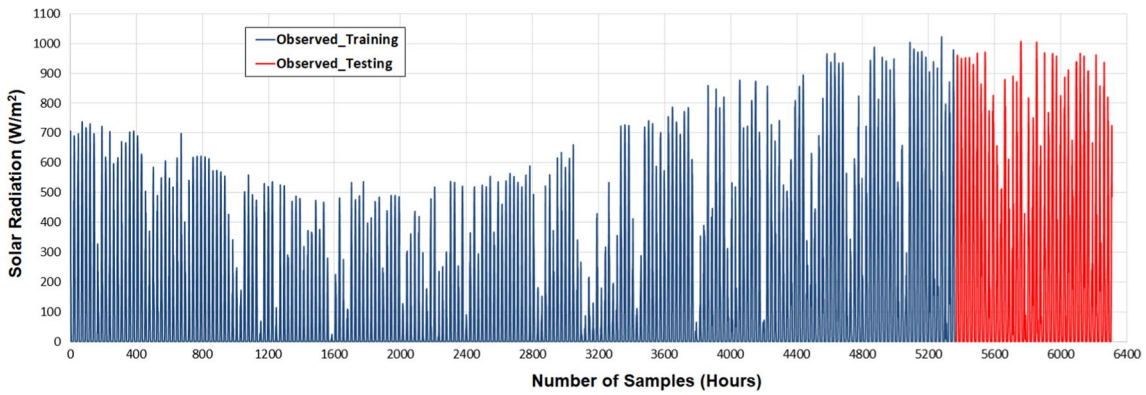

Fig. 6 Observed solar radiation, training (blue), and testing (red) data

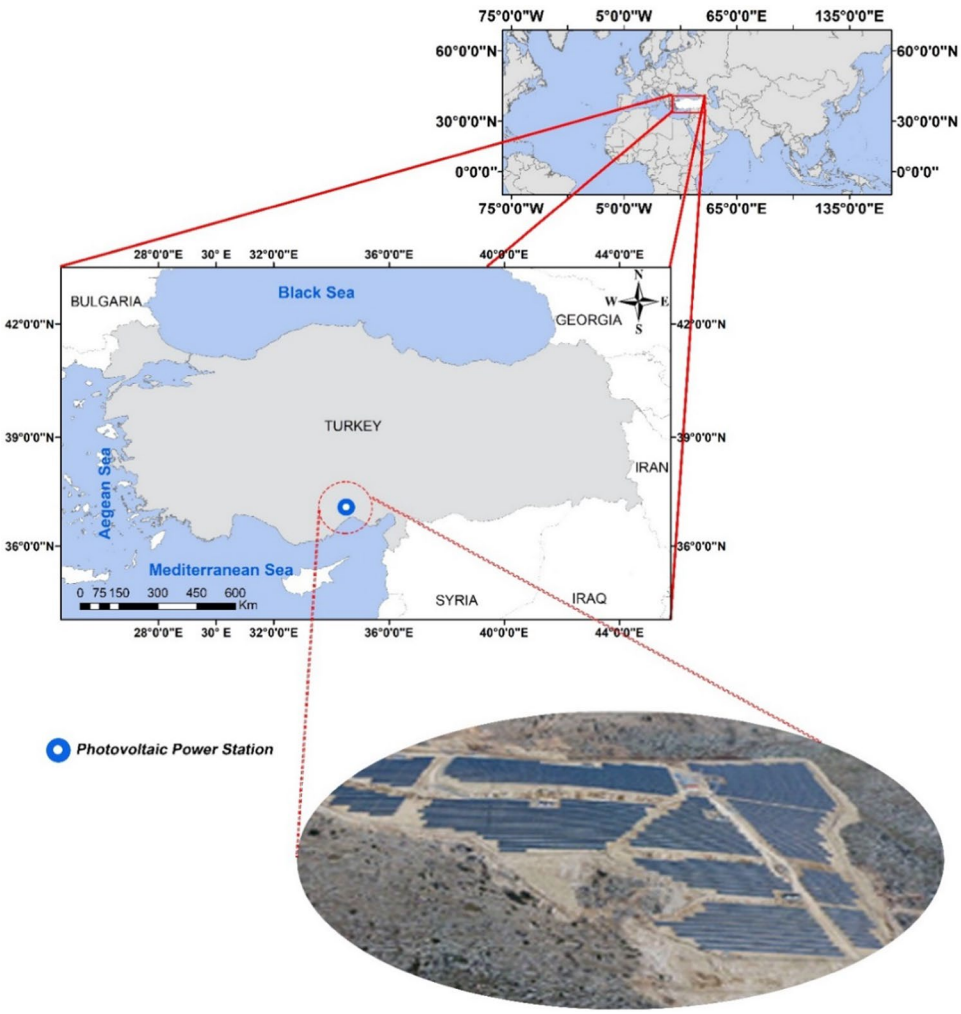

Fig. 7 The photovoltaic power station in Tarsus, Turkey

Table 1 Determination of optimal parameters for the prediction of solar radiation measured at Tarsus station using the ANFIS-FCM model

Number of MFs	Input number	Max epoch	MAE (W/m^2)	RMSE (W/m^2)	R
2	5	100	71.71	114.65	0.9320
3	5	100	68.10	112.01	0.9351
4	5	100	64.97	111.75	0.9355
5	5	100	63.96	110.87	0.9355
6	5	100	62.62	110.09	0.9357
7	5	100	61.81	110.24	0.9363
8	5	100	60.93	110.26	0.9370
8	**5**	**300**	**58.45**	**109.99**	**0.9372**
9	5	100	58.66	110.01	0.9371
10	5	100	58.77	110.46	0.9371
10	5	300	58.65	111.25	0.9353

The best results are bolded

The flow of information is input into the input layer and passes through output layers and the hidden layers to achieve the output information in the MLP network. Figure 2 shows a single-layer network of S logsig neurons with R inputs in the Feed-Forward Neural Network. The layer number is denoted by the superscript in the weight matrix for multi-layer networks. The appropriate notation is shown in Fig. 3 for the two-layer tansig/purelin feed-forward neural network.

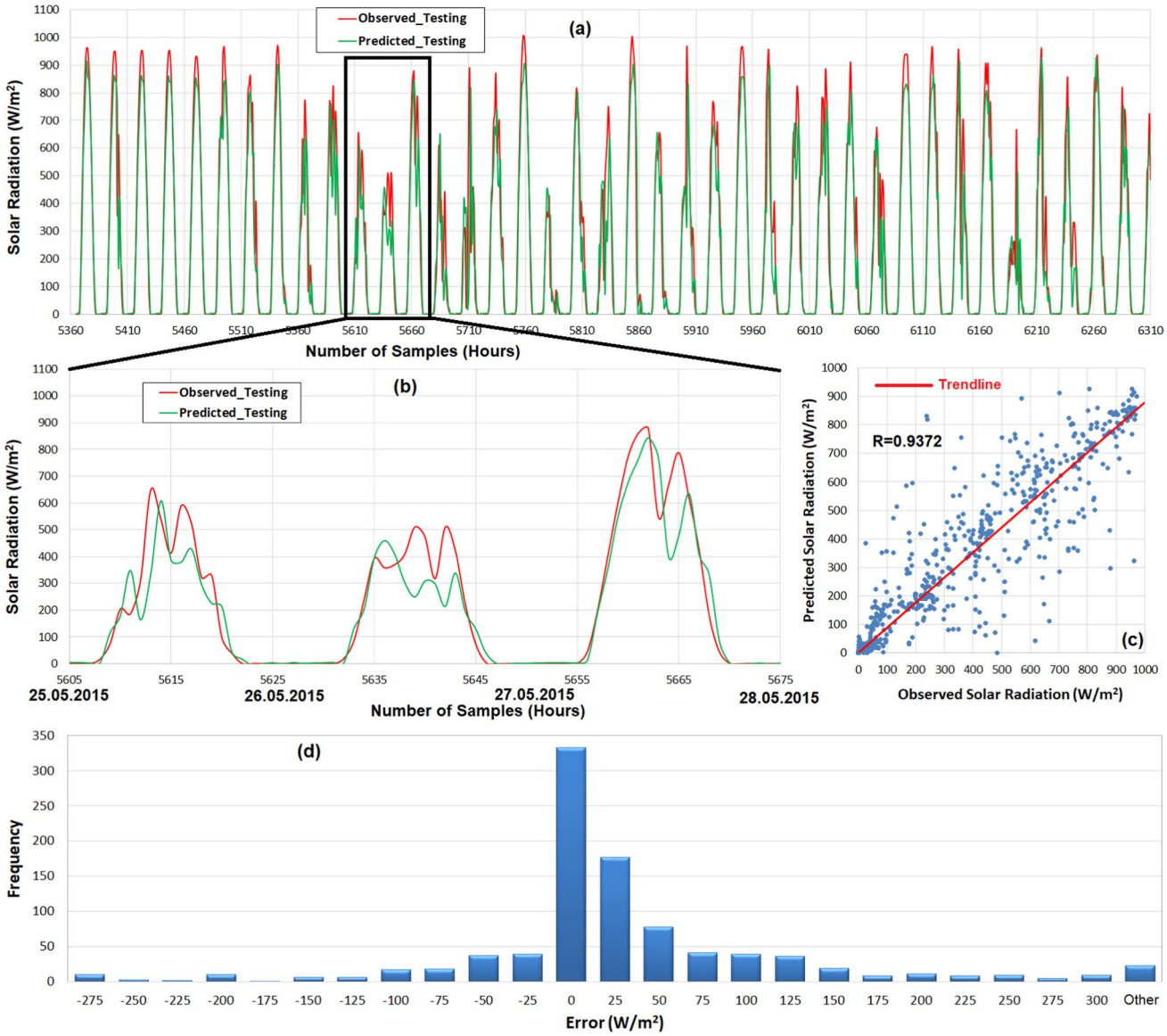

Fig. 8 ANFIS-FCM model for observed and predicted testing data between **a** 15 May 2015 and 24 June 2015, **b** 25–28 May 2015, **c** the observed versus predicted data for the model, **d** histogram of prediction errors for the model

2.3 Long short-term memory (LSTM) network

LSTMs use data from different times when processing sequential time-series data such as RNNs and are designed to avoid the problem of long-term dependence. The difference between LSTM and RNN is that LSTM nodes are structured differently. The RNN cell in the LSTM structure is also accompanied by memory. This memory allows previous time information to be received and transmitted the next time. The model can be trained to decide what information to get. Although these networks do not set out to learn how to remember information for long periods, it is the default behavior in practice. RNNs and LSTMs both have a chain-like structure (Temur 2019).

The LSTM architecture consists of sequential blocks that repeat each other as shown in Fig. 4. Generally, the LSTM structure consists of 3 different layers: input, output and hidden. Here, X_t represents the input data at time t and the output of the previous unit. h indicates the output of hidden units,

Table 2 Determination of optimal parameters for the prediction of solar radiation measured at Tarsus station using the ANFIS-GP model

Number of MFs	Max epoch	MAE (W/m^2)	RMSE (W/m^2)	R
2	100	78.17	164.96	0.8604
2	**300**	**78.17**	**164.96**	**0.8604**

The best results are bolded

and h_{t-1} indicates their previous output. In the figure, the red rectangle shows the neural network layers (Liu et al. 2021). The green circle represents point operations such as adding vectors. The line portion of the arrows carries the data in the node, and the head portions carry the data as input to other nodes. LSTM unit mathematical formulas and explanations are given in Fig. 5. Here, b_f, b_i, b_0, b_g are bias vectors.

2.4 Error analysis

Accuracy is clearly the most significant criterion in the evaluation of the performance success of the prediction methods. Therefore, in this study, commonly used error metrics in solar radiation estimation were used in the literature (Bamisile et al. 2020; Li et al. 2021). Used error metrics are denoted by the abbreviations MAE, RMSE, and R, which correspond to mean absolute error, root mean square error, and correlation coefficient, respectively. The MAE determines the average size

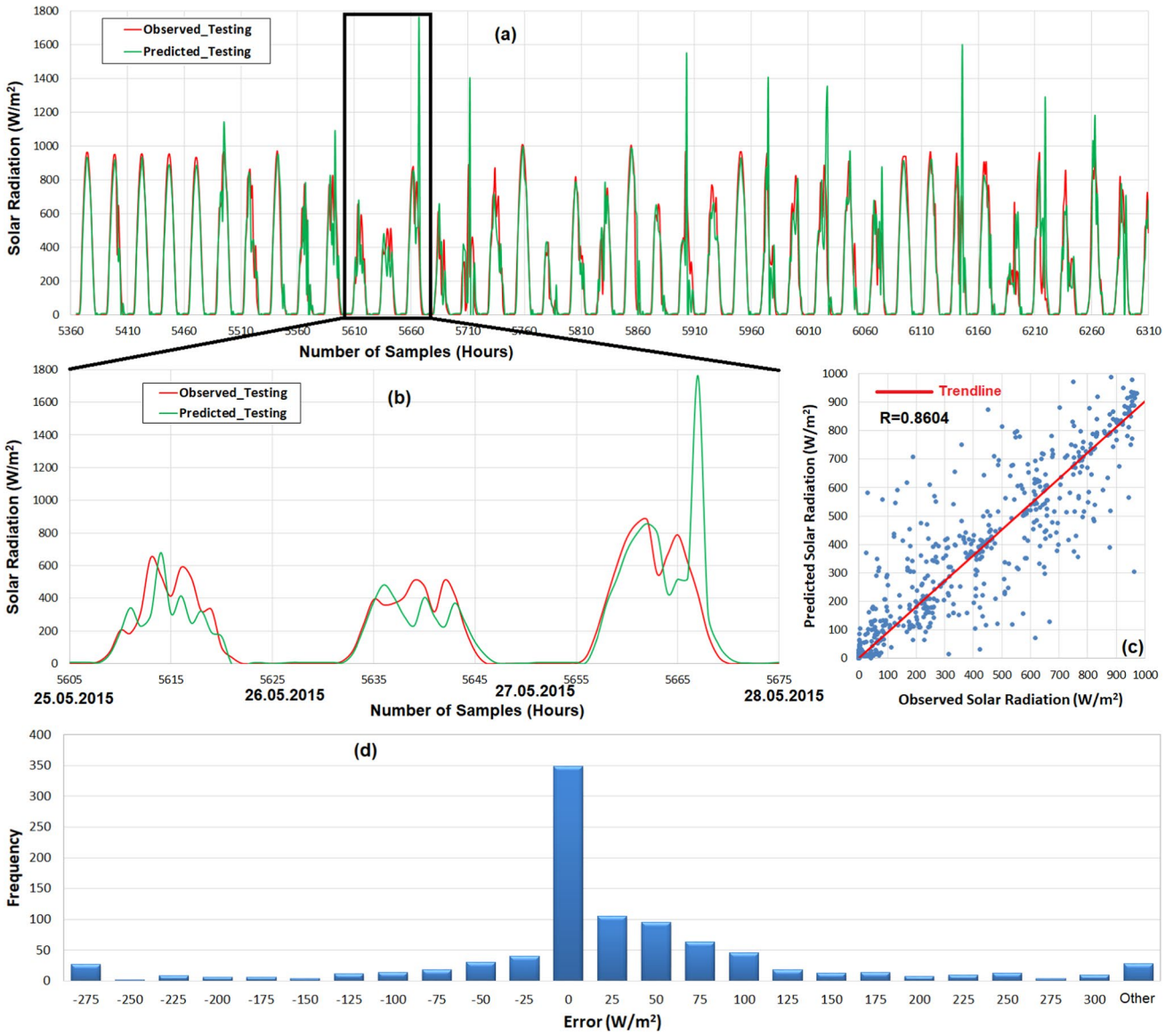

Fig. 9 ANFIS-GP model for observed and predicted testing data between **a** 15 May 2015 and 24 June 2015, **b** 25–28 May 2015, **c** the observed versus predicted data for the model, **d** histogram of prediction errors for the model

Table 3 Determination of optimal parameters for the prediction of solar radiation measured at Tarsus station using the MLP model

Input Number	Number of Neurons	Max Iteration	MAE (W/m^2)	RMSE (W/m^2)	R
5	5	300	64.37	110.91	0.9346
5	**6**	**300**	**61.68**	**108.72**	**0.9391**
5	7	300	62.57	110.12	0.9367
5	8	300	63.62	109.72	0.9376
5	9	300	63.02	110.01	0.9363
5	10	300	62.91	111.43	0.9347

The best results are bolded

of errors in a set of estimates without taking into account the direction of overestimation or underestimation. It is appropriate for determining the accuracy of continuous variables. It is possible to diagnose error variation in a variety of estimates using together RMSE and MAE.

In this study, these error criteria were used to assess the accuracy of a model in predicting an observed output variable. Their calculation methods are, respectively, provided as follows (Chaudhuri and Middey 2011; Bilgili et al. 2021):

$$MAE = \frac{1}{N}\sum_{i=1}^{N}|p(i) - o(i)| \tag{13}$$

$$RMSE = \sqrt{\frac{1}{N}\sum_{i=1}^{N}\left[p(i) - o(i)\right]^2} \tag{14}$$

$$R = \left(\sum_{i=1}^{N}\left[p(i) - \overline{p}\right]\left[o(i) - \overline{o}\right]\right) \Big/ \left(\sqrt{\sum_{i=1}^{N}\left[p(i) - \overline{p}\right]^2}\sqrt{\sum_{i=1}^{N}\left[o(i) - \overline{o}\right]^2}\right) \tag{15}$$

The p(i) designation and o(i) assignment in these equations denote predicted and observed values at time I, respectively. Furthermore, the terms $\overline{p}$ and $\overline{o}$ represent the averages of the predicted and actual values, respectively, while N represents the total number of data points.

3 Results and discussion

3.1 Data and study area

The main aim of the study is to present the best method based on the clustered ANFIS-GP, ANFIS-FCM, MLP and LSTM approaches for 1-h-ahead solar radiation forecasting. Figure 6 shows the testing and training time series with hourly SR data observed for proposed methods. For 1-h, ahead of short-term SR prediction, the 1-h intervals SR data set from October 10, 2014, to May 16, 2015, was used. The 6382 samples acquired were separated into 2 groups (5436 data representing 85% of the training set and 946 data representing 15% of the test set). The solar radiation dataset for 9 months was collected from the solar-PV power plant in Tarsus/Turkey. In Tarsus city, the total amount of solar energy measured per year was 1900 (kWh/m^2), the average monthly solar energy amount was 158 (kWh/m^2) and the sunshine duration was 2900 (hours/year) per year. Due to this high solar potential, the city of Tarsus is a very suitable region for solar energy. Figure 7 illustrates the general overview of the study area and the solar-PV power plant station where the measurement is taken. The solar-PV power plant's geographic coordinates are 34°45′37 "E and 37°07′19"N. The observation spectral range of the pyranometer is between 285 and 2800 nm and the range of measure is between 0 and 2000 W/m^2.

3.2 Results for ANFIS-FCM method

Determination of optimal parameters for the prediction of SR using the ANFIS-FCM method from the Tarsus station is shown in Table 1. This table shows the best results in bold. First, this clustering model was chosen, and various input, clusters, and epoch numbers were used in the simulation. The performance of the method was determined by calculating RMSE, MAE, and R-values. For this method, the number of MFs used ranged from 2 to 10. The quality metrics varied from 58.45 W/m^2 to 71.71 W/m^2 (MAE), 109.99 W/m^2 to 114.65 W/m^2 (RMSE), and 0.9320 to 0.9372 (R), respectively. The best-obtained R is 0.9372 for MF = 8 in ANFIS-FCM. The results of a low number of clusters are unsatisfactory.

The hourly SR data (black) at solar-PV with observed (red) and predicted values for ANFIS-FCM (green) methods are presented in Fig. 8a. Figure 8b shows 2 days of zoomed data between 25.05.2015 and 28.05.2015. SR data regression graphs displaying observed and predicted values from the ANFIS-FCM method were given in Fig. 8c. From Fig. 8a, b and c, the predicted SR data almost perfectly fit the observed values for the

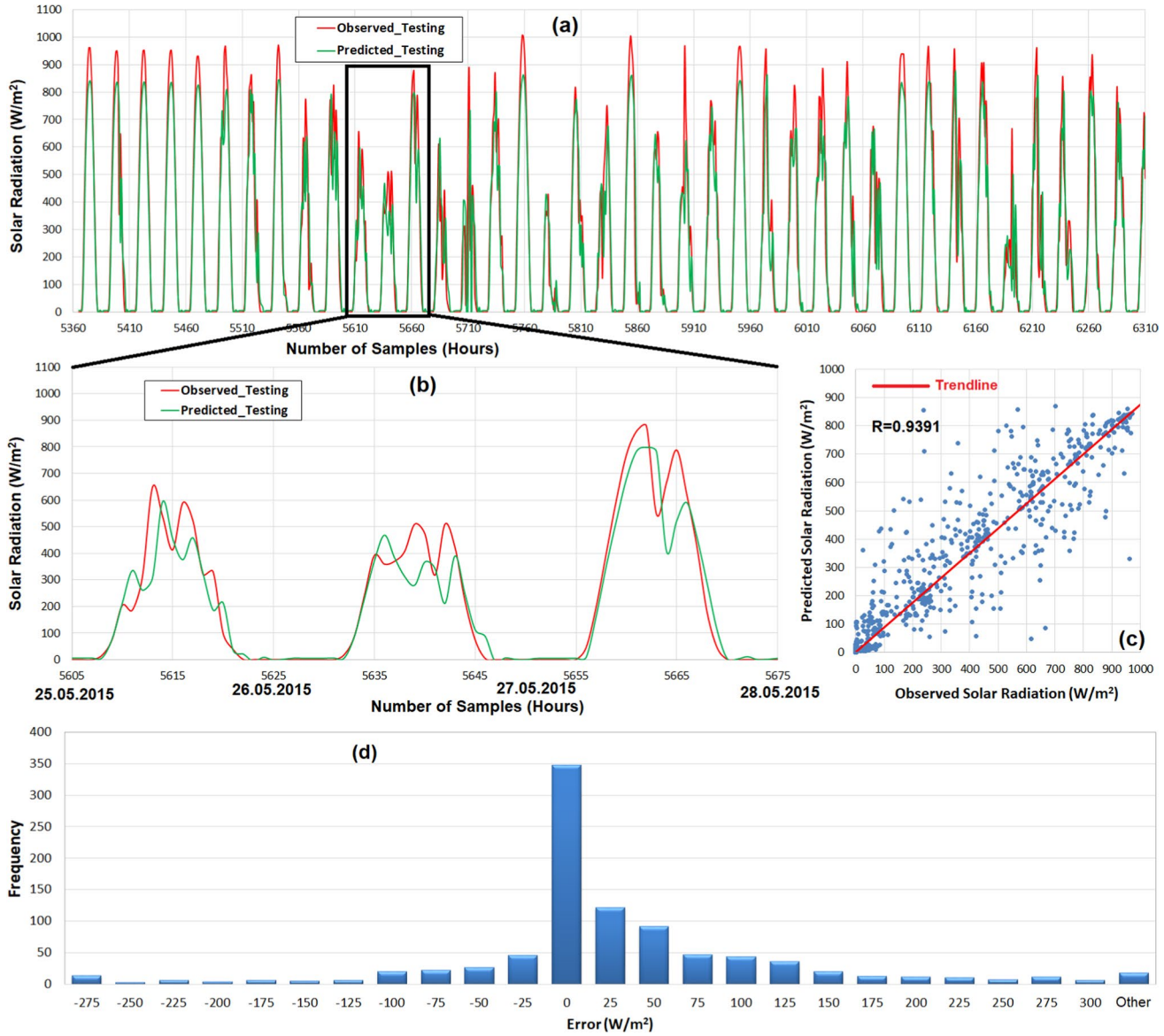

Fig. 10 MLP model for observed and predicted testing data between **a** 15 May 2015 and 24 June 2015, **b** 25–28 May 2015, **c** the observed versus predicted data for the model, **d** histogram of prediction errors for the model

ANFIS-FCM method. ANFIS-FCM histogram plot of the prediction of SR values is indicated in Fig. 8d. The results in that model appear to be skewed to the positive. More than 82% of the model predictions have an error $\leq \pm 100$ W/m^2 for the ANFIS-FCM method as can be seen in this figure.

3.3 Results for ANFIS-GP method

Table 2 points out the determination of optimal parameters for the prediction of SR using the ANFIS-GP method from the Tarsus station. RMSE, MAE, and R-values were calculated to show the performance of the method. The number of MFs and epoch numbers can be seen in this table. For 100 and 300 epoch numbers, it is seen that all the statistical quality metrics for this method show the same results. The best quality metrics were 78.17 W/m^2 (MAE), 164.96 W/m^2 (RMSE), and 0.8604 (R), respectively. In ANFIS-GP, the best R obtained is 0.8604 for MF = 2.

Figure 9a shows all observed data (red) and predicted data (green) for the hourly SR data of the Tarsus station. Figure 9b reveals the zoom in the original SR values with red and the predicted SR values with green. The regression plot of the observed and predicted daily SR is given in Fig. 9c. This figure reveals the distribution of the data. The R, equal to 0.8604, proves the good fit of the observed

Table 4 Determination of optimal parameters for the prediction of solar radiation measured at Tarsus station using the LSTM model

Hidden layer number	Epoch Number	MAE (W/m^2)	RMSE (W/m^2)	R
5	300	55.41	102.21	0.9453
10	300	55.32	101.88	0.9457
20	300	55.24	101.96	0.9451
30	300	54.86	102.05	0.9446
50	300	54.30	102.10	0.9451
75	300	53.81	101.83	0.9454
100	**300**	**53.37**	**101.20**	**0.9459**
100	500	53.45	101.57	0.9457
150	300	53.55	101.63	0.9453
175	300	53.79	101.65	0.9456
200	300	53.75	101.66	0.9448
300	300	53.68	101.59	0.9450

The best results are bolded

and predicted data. However, this model gave the worst statistical values among other models. Figure 9d represents the ANFIS-GP histogram plot of the prediction of SR values. The results in that model also appear to be skewed to the positive. As seen in this figure, more than 80% of the model predictions have an error $\leq \pm 100$ W/m^2 for the ANFIS-GP model.

3.4 Results for MLP method

The statistical performance metrics of the hourly SR forecasting for the MLP method are shown in Table 3. The number of neurons was varied between 5 and 10 for the MLP method. The quality metrics varied from 61.68 W/m^2 to 64.37 W/m^2 (MAE), 108.72 W/m^2 to 111.43 W/m^2 (RMSE) and 0.9346 to 0.9391 (R), respectively. In the MLP method, the best MAE value of 61.68 W/m^2 was obtained when the number of neurons was 2.

Figure 10a shows testing time series with observed (red) and predicted (green) hourly SR data for the MLP method. Figure 10b shows 3 days of zoomed data between 25.05.2015 and 28.05.2015. SR data regression graphs displaying observed and predicted values from the MLP method are given in Fig. 10c. A histogram plot of the prediction of SR values obtained using the MLP model can be seen in Fig. 10d. The results in that model also appear to be skewed to the positive. More than 81% of the model predictions have an error of $\leq \pm 100$ W/m^2 for the MLP model can be seen in this figure.

3.5 Results for LSTM method

Table 4 lists the various evaluation criteria for the LSTM model. To demonstrate the method's performance, the MAE, RMSE, and R-values were calculated. Regarding the LSTM method, this model gave almost similar results in terms of evaluation criteria. This table shows the epoch number and the influence of the hidden layer number. 300 epoch numbers and 100 hidden layers gave the best results. The lowest RMSE is equal to 101.2 W/m^2 and MAE is 53.57 W/m^2 with an R-value of 0.9459. Increasing the hidden layers numbers and epoch numbers together reduced the RMSE and MAE values.

Figure 11a illustrates the hourly measured SR for the Tarsus station used for the testing stage. It is seen that the SR values of observed and predicted values are consistent with one another, with only minor differences between the values of each data. Figure 11b shows 3 days of zoomed data between 25.05.2015 and 28.05.2015. The validity of obtained results can be seen in Fig. 11b where is shown good correlation between the calculated and observed hours SR. From Figs. 11a, b and c, it is seen that the predicted SR data almost overlap with the observed values for the LSTM method. According to the figures, the LSTM neural network achieved the best model fit data, followed by the ANFIS-FCM model. Figure 11d represents the LSTM histogram plot of the prediction of SR values. The results in that model similarly appear to be skewed to the positive. As seen in this figure, more than 84% of the model predictions have an error $\leq \pm 100$ W/m^2 for that model.

3.6 Comparison of models

In this section, an extensive comparison of the proposed LSTM model to the ANNFIS-FCM, ANFIS-GP, and MLP models was performed. To summarize, Table 5 emphasizes the statistical accuracy results of hourly SR predictions. In comparison to the other models, the results show that the LSTM yielded the lowest values of MAE (53.37 W/m^2), RMSE (101.20 W/m^2), and exhibited the higher values of the R (0.9459). The nearest competitor of LSTM is MLP according to RMSE and R-values. Moreover, in terms of MAE, the ANFIS-FCM models are better than the ANFIS-GP and MLP models. The ANFIS-GP performed worse than the other recommended models. In addition, Fig. 12 shows comparison of proposed models with observed values and Taylor diagram for assessing the performance of proposed models. Based on the RMSE and Taylor diagram, the ranking was: LSTM (the method with the best performance, with RMSE = 101.20 W/m^2) > MLP > ANFIS-FCM > ANFIS-GP (the worst predictive method with RMSE = 164.96 W/m^2). Overall, based on the Taylor diagram and, three statistical

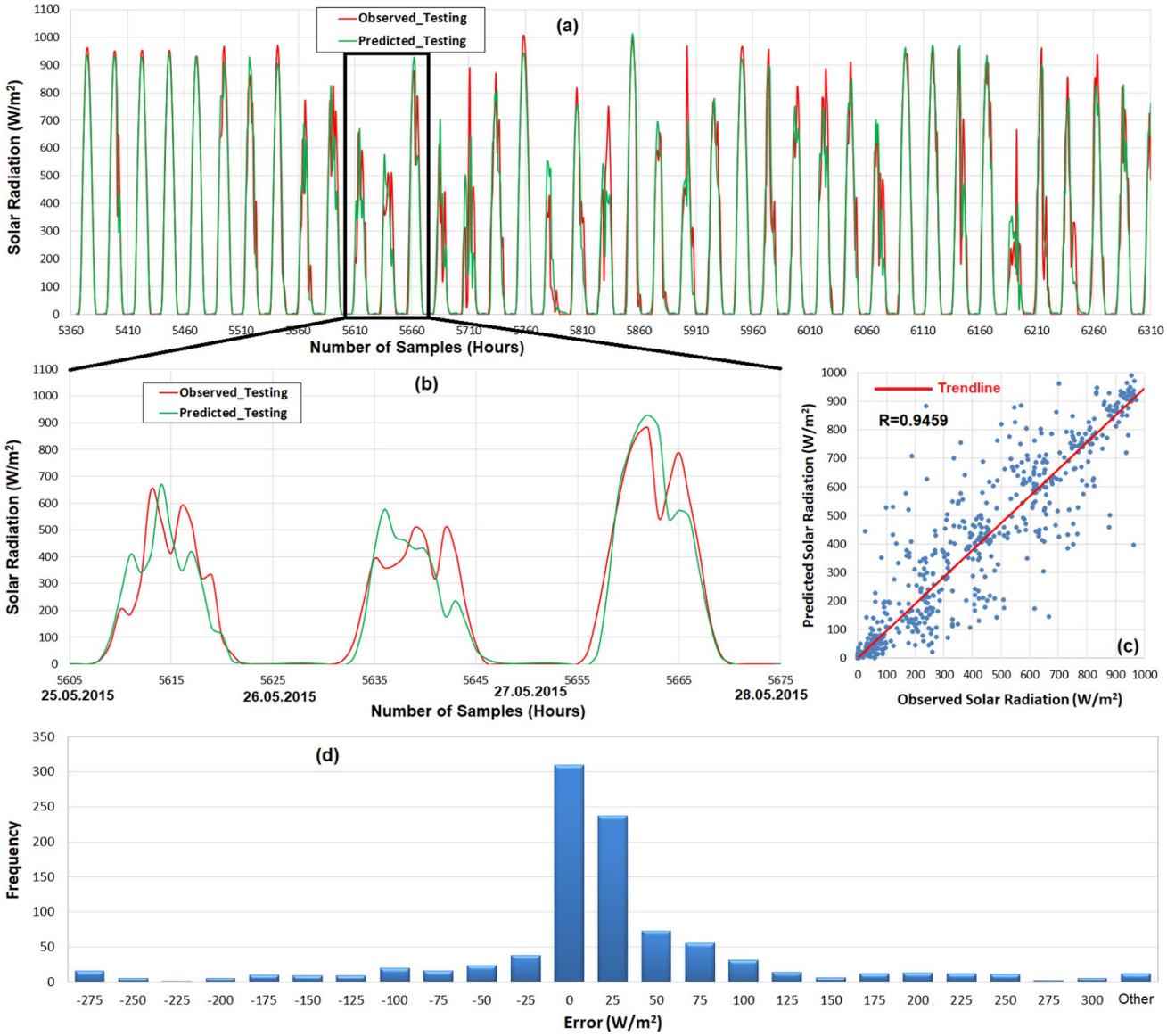

Fig. 11 LSTM model for observed and predicted testing data between **a** 15 May 2015 and 24 June 2015, **b** 25–28 May 2015, **c** the observed versus predicted data for the model, **d** histogram of prediction errors for the model

Table 5 Each model's prediction performance

Model	MAE (W/m^2)	RMSE (W/m^2)	R
LSTM	**53.37**	**101.20**	**0.9459**
ANFIS-FCM	58.45	109.99	0.9372
ANFIS-GP	78.17	164.96	0.8604
MLP	61.68	108.72	0.9391

The best results are bolded

criteria; the LSTM model is the most accurate among the other proposed models.

3.7 Comparison with other models

Although there are a lot of studies on SR forecasting in the literature, there are few on the forecasting of short-term hourly SR time series. Nonetheless, the proposed method's forecasting results are compared to those obtained from some published studies based on hourly SR estimates, as given in Table 6. Time-series data values are used to forecast future values based on historical data points. Our proposed methods and many of the studies listed have used time-series data. Most of the studies using the time series in Table 6 have obtained successful estimation results. Few studies in the list did not use time series (Jiménez-Pérez and Mora-López 2016; Suyono et al. 2018; Chen et al. 2019). Hourly SR

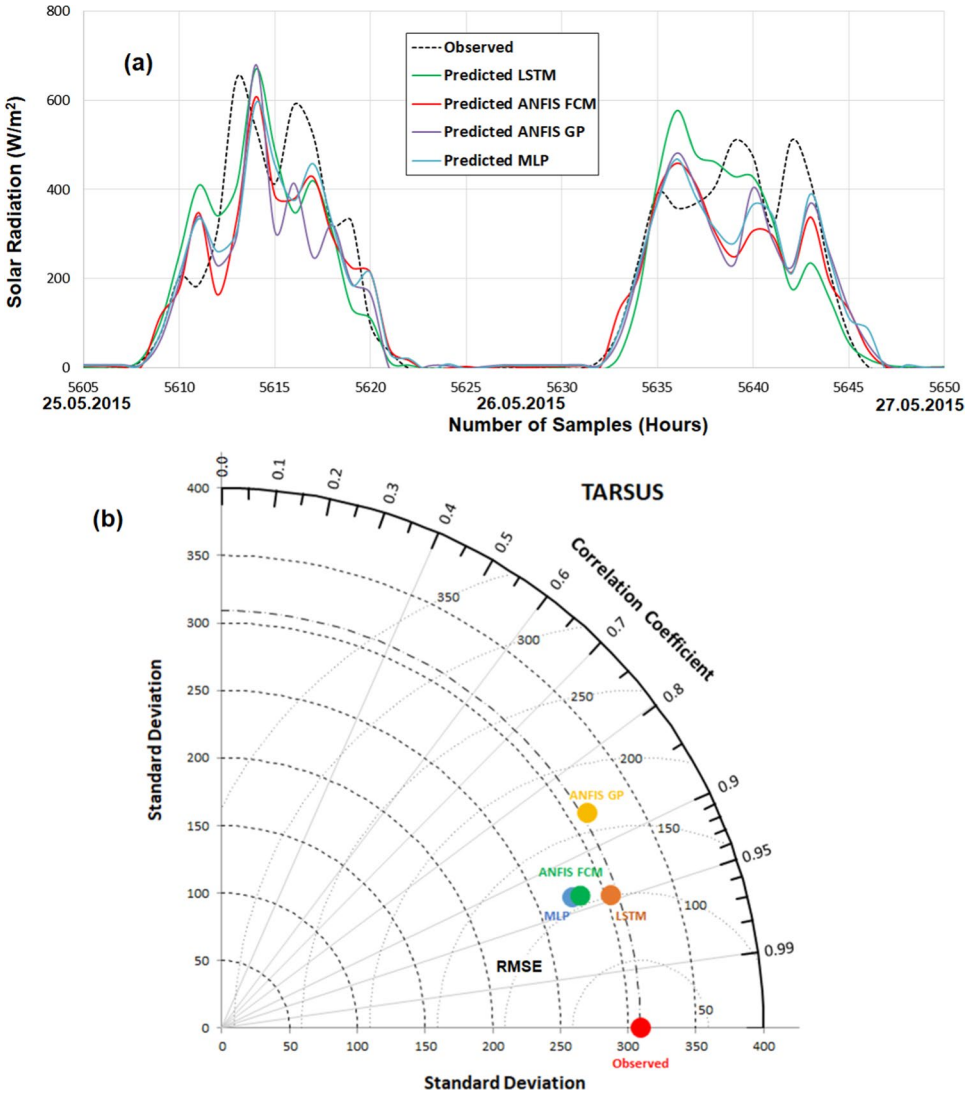

Fig. 12 **a** Comparison of proposed models with observed values. **b** Taylor diagram for assessing the performance of proposed models

prediction is a dynamic system and statistical methods and numerical methods cannot estimate the targets with the high accuracy. For instance, as shown in Table 6, Ref. (Suyono et al. 2018) reported approximately RMSE = 148.7 W/m^2 for statistical methods, in addition, Ref. (de Araujo 2020) calculated the RMSE value as 210 W/m^2 with numerical methods, order to forecast SR. However, other studies have demonstrated that machine learning and hybrid methods are highly effective at predicting this system. Our ANFIS methods and Ref. (Benmouiza and Cheknane 2019) gave similar results in term of prediction. Except ANFIS-GP, ANFIS methods showed the second best performance in the list. The worst estimation result was obtained with the numeric WRF method (de Araujo 2020). The results illustrate the fact that the LSTM model has lower RMSE values, which shows that LSTM performs better than other methods in SR prediction.

LSTM is capable of analyzing data and learning long-term dependencies, especially in sequence prediction problems. Aside from single data and images, it can process the entire data sequence. This aids in speech recognition, machine translation, and other applications. In addition, the LSTM model is capable to learn the long-term dependencies and temporal and spatial patterns of solar radiation data, which helps to exploit the contextual information. Therefore, these unique capabilities have enabled the LSTM model to yield better results.

4 Conclusion

Since SR-based power plants produce fluctuating amounts of electricity, integrating them into the grid is a difficult task. Thus, accurate SR forecasting is critical for grid-connected solar power plant efficiency. In this study, ANFIS–FCM, ANFIS-GP, MLP, and LSTM neural network models were proposed for 1-h-ahead SR prediction. The applicability and

Table 6 Performance for predicting hourly solar radiation from literature review

Ref	Model	Location	Input	RMSE (W/m^2)	R
de Araujo (2020)	WRF	Gifu/Japan	Time-series SR past data	210	–
Benmouiza and Cheknane (2019)	ANFIS-FCM	Ghardaia, Algeria	Time-series SR past data	112	–
Benmouiza and Cheknane (2019)	ANFIS-SC	Ghardaia, Algeria	Time-series SR past data	121	–
Benmouiza and Cheknane (2019)	ANFIS-GP	Ghardaia, Algeria	Time-series SR past data	155	–
Benmouiza and Cheknane (2013)	K-Means and NAR	Oran/Algeria	Time series SR past data		0.9330
Huang et al. (2013)	CARDS	Victoria, Australia	Time-series SR past data	146	–
Benmouiza et al. (2016)	ARMA + NAR	Ghardaia, Algeria	Time-series SR past data	122	–
Shamim et al. (2015)	BFGS-ANN	Brue, England	Time-series SR and meteorological past data	170.9	0.8010
Jiménez-Pérez and Mora-López (2016)	SVM-C + SVM-R	Malaga, Spain	SR and various meteorological past data	119	–
Chen et al. (2019)	ANN	Hong Kong	Various meteorological data	117.3	0.9066
Wu and Wang (2016)	DirRec-BP	3 sites in America	Time-series SR past data	162.91	
Wu and Wang (2016)	DirRec-SOM-OPELM	3 sites in America	Time-series SR past data	128.9	–
Wu and Wang (2016)	ARIMA	3 sites in America	Time-series SR past data	134.86	–
Suyono et al. (2018)	MLR	Basel, Switzerland	Various meteorological data	148.27	
Suyono et al. (2018)	ANFIS	Basel, Switzerland	Various meteorological data	138.35	
Che et al. (2019)	WRF	Qinghai, China	Time-series SR past data	158.1	
Our model	ANFIS-GP	Tarsus/Turkey	Time-series SR past data	164.96	0.8604
Our model	ANFIS-FCM	Tarsus/Turkey	Time-series SR past data	109.99	0.9372
Our model	MLP	Tarsus/Turkey	Time-series SR past data	108.2	0.9391
Our model	LSTM	Tarsus/Turkey	Time-series SR past data	101.2	0.9459

validity of the proposed approaches are extensively evaluated using actual data from the solar-PV power plant in Turkey. The total of 6382 hourly data was divided into two parts 85% training set and 15% testing set for all methods. Overall, it has successfully demonstrated that proposed models generally outperform in modeling SR with limited data (only SR data), and this is especially useful in areas where other climatic variables are unavailable. However, among all methods, LSTM performs good robustness and has high prediction accuracy for all evaluation criteria. The RMSE values of LSTM (101.20 W/m^2), MLP (108.72 W/m^2), ANFIS-FCM (109.99 W/m^2), and ANFIS-GP (164.96 W/m^2) for hourly predictions, respectively, demonstrate the highest performance of LSTM compared to the other proposed models.

Generally, the results of this study show that the proposed methods are effective in predicting short-term hourly SR under various climatic circumstances. Therefore, engineers and researchers can use the findings of this study to improve solar power plant modeling and planning. For future research, the proposed prediction system based on the LSTM model can be applied to various domains including wave energy and load characterization to help policymakers manage freely available energy resources more efficiently and effectively.

Acknowledgements We had like to thank Pilye Energy Cons. Ind. and Trading Co., generously allowed us to use solar radiation data in our study.

Funding No funds, grants or other support was received.

Data availability All the data generated or analyzed in the current study are available from the corresponding author on reasonable request.

Declarations

Conflict of interest The authors have no relevant financial or nonfinancial interest to disclose.

References

Abdulkarim HT, Sansom CL, Patchigolla K, King P (2020) Statistical and economic analysis of solar radiation and climatic data for the development of solar PV system in Nigeria. Energy Rep 6:309–316. https://doi.org/10.1016/j.egyr.2019.08.061

Abdulshahed AM, Longstaff AP, Fletcher S, Myers A (2015) Thermal error modelling of machine tools based on ANFIS with fuzzy c-means clustering using a thermal imaging camera. Appl Math Model 39:1837–1852. https://doi.org/10.1016/j.apm.2014.10.016

Abonyi J, Andersen H, Nagy L, Szeifert F (1999) Inverse fuzzy-process-model based direct adaptive control. Math Comput Simul 51:119–132. https://doi.org/10.1016/s0378-4754(99)00142-1

Adeleke O, Akinlabi S, Jen TC et al (2022) Evolutionary-based neuro-fuzzy modelling of combustion enthalpy of municipal solid waste.

Neural Comput Appl 34:7419–7436. https://doi.org/10.1007/s00521-021-06870-2
Aguinaga A, Luo X, Hidalgo V et al (2017) A feed-forward backpropagation neural network method for remaining useful life prediction of Francis turbines. Proc World Congr Mech Chem Mater Eng. https://doi.org/10.11159/icmie17.126
Akhter MN, Mekhilef S, Mokhlis H, Shah NM (2019) Review on forecasting of photovoltaic power generation based on machine learning and metaheuristic techniques. IET Renew Power Gener 13:1009–1023. https://doi.org/10.1049/iet-rpg.2018.5649
Ali-Ou-Salah H, Oukarfi B, Bahani K, Moujabbir M (2021) A new hybrid model for hourly solar radiation forecasting using daily classification technique and machine learning algorithms. Math Probl Eng. https://doi.org/10.1155/2021/6692626
Azizi A, Izadfar HR (2019) A novel ANFIS-based MPPT controller for two-switch flyback inverter in photovoltaic systems. J Renew Sustain Energy. https://doi.org/10.1063/1.5082736
Bamisile O, Oluwasanmi A, Obiora S et al (2020) Application of deep learning for solar irradiance and solar photovoltaic multi-parameter forecast. Energy Sources, Part A Recover Util Environ Eff 00:1–21. https://doi.org/10.1080/15567036.2020.1801903
Benmouiza K, Cheknane A (2013) Forecasting hourly global solar radiation using hybrid k-means and nonlinear autoregressive neural network models. Energy Convers Manag 75:561–569. https://doi.org/10.1016/j.enconman.2013.07.003
Benmouiza K, Cheknane A (2019) Clustered ANFIS network using fuzzy c-means, subtractive clustering, and grid partitioning for hourly solar radiation forecasting. Theor Appl Climatol 137:31–43. https://doi.org/10.1007/s00704-018-2576-4
Benmouiza K, Tadj M, Cheknane A (2016) Classification of hourly solar radiation using fuzzy c-means algorithm for optimal standalone PV system sizing. Int J Electr Power Energy Syst 82:233–241. https://doi.org/10.1016/j.ijepes.2016.03.019
Bezdek CJ (2003) Pattern Recognition with Fuzzy Objective Function Algorithms. PLENUM PRESS, NEW YORK
Bilgili M, Ozgoren M (2011) Daily total global solar radiation modeling from several meteorological data. Meteorol Atmos Phys 112:125–138. https://doi.org/10.1007/s00703-011-0137-9
Bilgili M, Yildirim A, Ozbek A et al (2021) Long short-term memory (LSTM) neural network and adaptive neuro-fuzzy inference system (ANFIS) approach in modeling renewable electricity generation forecasting. Int J Green Energy 18:578–594. https://doi.org/10.1080/15435075.2020.1865375
Çakin E (2019) Analysis of the relationship between the personal characteristics and entrepreneurship potential with adaptive network based fuzzy inference system (anfis)
Chaudhuri S, Middey A (2011) Adaptive neuro-fuzzy inference system to forecast peak gust speed during thunderstorms. Meteorol Atmos Phys 114:139–149. https://doi.org/10.1007/s00703-011-0158-4
Che Y, Chen L, Zheng J et al (2019) A novel hybrid model of WRF and clearness index-based kalman filter for day-ahead solar radiation forecasting. Appl Sci 9:1–16. https://doi.org/10.3390/app9193967
Chen JL, Li GS (2014) Evaluation of support vector machine for estimation of solar radiation from measured meteorological variables. Theor Appl Climatol 115:627–638. https://doi.org/10.1007/s00704-013-0924-y
Chen W, Li DH, Li S, Lam JC (2019) Estimating hourly global solar irradiance using artificial neural networks - A case study of Hong Kong. IOP Conf Ser Mater Sci Eng. https://doi.org/10.1088/1757-899X/556/1/012043
Chen X, Huang J, Han Z et al (2020) The importance of short lag-time in the runoff forecasting model based on long short-term memory. J Hydrol 589:125359. https://doi.org/10.1016/j.jhydrol.2020.125359
Dhakal S, Gautam Y, Bhattarai A (2020) Evaluation of temperature-based empirical models and machine learning techniques to estimate daily global solar radiation at biratnagar airport. Nepal Adv Meteorol. https://doi.org/10.1155/2020/8895311
de Araujo JMS (2020) Performance comparison of solar radiation forecasting between WRF and LSTM in Gifu. Japan Environ Res Commun 2:045002. https://doi.org/10.1088/2515-7620/ab7366
Dinçer F (2011) Türkiye'de Güneş Enerjisinden Elektrik Üretimi Potansiyeli - Ekonomik Analizi ve AB Ülkeleri ile Karşılaştırmalı Değerlendirme. Kahramanmaras Sutcu Imam Univ J Eng Sci 14:8–17. https://doi.org/10.17780/KSUJES.10191
Dunn JC (1973) A fuzzy relative of the ISODATA process and its use in detecting compact well-separated clusters. J Cybern 3:32–57. https://doi.org/10.1080/01969727308546046
Ghimire S, Deo RC, Raj N, Mi J (2019) Deep solar radiation forecasting with convolutional neural network and long short-term memory network algorithms. Appl Energy 253:113541. https://doi.org/10.1016/j.apenergy.2019.113541
Guermoui M, Melgani F, Gairaa K, Mekhalfi ML (2020) A comprehensive review of hybrid models for solar radiation forecasting. J Clean Prod 258:120357. https://doi.org/10.1016/j.jclepro.2020.120357
Huang J, Korolkiewicz M, Agrawal M, Boland J (2013) Forecasting solar radiation on an hourly time scale using a Coupled AutoRegressive and Dynamical System (CARDS) model. Sol Energy 87:136–149. https://doi.org/10.1016/j.solener.2012.10.012
Huynh ANL, Deo RC, An-Vo DA et al (2020) Near real-time global solar radiation forecasting at multiple time-step horizons using the long short-term memory network. Energies. https://doi.org/10.3390/en13143517
IRENA (2021) Offshore renewables: An action agenda for deployment
Jang JSR (1993) ANFIS: Adaptive-Network-Based Fuzzy Inference System. IEEE Trans Syst Man Cybern 23:665–685. https://doi.org/10.1109/21.256541
Jiménez-Pérez PF, Mora-López L (2016) Modeling and forecasting hourly global solar radiation using clustering and classification techniques. Sol Energy 135:682–691. https://doi.org/10.1016/j.solener.2016.06.039
Kim S, Seo Y, Rezaie-Balf M et al (2019) Evaluation of daily solar radiation flux using soft computing approaches based on different meteorological information: peninsula vs continent. Theor Appl Climatol 137:693–712. https://doi.org/10.1007/s00704-018-2627-x
Kumari P, Toshniwal D (2021) Long short term memory–convolutional neural network based deep hybrid approach for solar irradiance forecasting. Appl Energy 295:117061. https://doi.org/10.1016/j.apenergy.2021.117061
Li X, Peng L, Yao X et al (2017) Long short-term memory neural network for air pollutant concentration predictions: Method development and evaluation. Environ Pollut 231:997–1004. https://doi.org/10.1016/j.envpol.2017.08.114
Li C, Zhang Y, Zhao G, Ren Y (2021) Hourly solar irradiance prediction using deep BiLSTM network. Earth Sci Informatics 14:299–309. https://doi.org/10.1007/s12145-020-00511-3
Linares-Rodriguez A, Ruiz-Arias JA, Pozo-Vazquez D, Tovar-Pescador J (2013) An artificial neural network ensemble model for estimating global solar radiation from Meteosat satellite images. Energy 61:636–645. https://doi.org/10.1016/j.energy.2013.09.008
Liu H, He B, Qin P et al (2021) Sea level anomaly intelligent inversion model based on LSTM-RBF network. Meteorol Atmos Phys 133:245–259. https://doi.org/10.1007/s00703-020-00745-2
Ma X, Tao Z, Wang Y et al (2015) Long short-term memory neural network for traffic speed prediction using remote microwave sensor data. Transp Res Part C Emerg Technol 54:187–197. https://doi.org/10.1016/j.trc.2015.03.014
Mirbolouki A, Heddam S, Singh Parmar K et al (2022) Comparison of the advanced machine learning methods for better prediction

accuracy of solar radiation using only temperature data: A case study. Int J Energy Res 46:2709–2736. https://doi.org/10.1002/er.7341

Moghaddamnia A, Remesan R, Kashani MH et al (2009) Comparison of LLR, MLP, Elman, NNARX and ANFIS Models-with a case study in solar radiation estimation. J Atmos Solar-Terrestrial Phys 71:975–982. https://doi.org/10.1016/j.jastp.2009.04.009

Mohammadi K, Shamshirband S, Kamsin A et al (2016) Identifying the most significant input parameters for predicting global solar radiation using an ANFIS selection procedure. Renew Sustain Energy Rev 63:423–434. https://doi.org/10.1016/j.rser.2016.05.065

Naderloo L (2020) Prediction of solar radiation on the horizon using neural network methods, ANFIS and RSM (case study: Sarpol-e-Zahab Township, Iran). J Earth Syst Sci. https://doi.org/10.1007/s12040-020-01414-z

Obiora CN, Ali A, Hasan AN (2020) Forecasting Hourly Solar Irradiance Using Long Short-Term Memory (LSTM) Network. 11th Int Renew Energy Congr IREC 2020. doi:https://doi.org/10.1109/IREC48820.2020.9310449

Ozgoren M, Bilgili M, Sahin B (2012) Estimation of global solar radiation using ANN over Turkey. Expert Syst Appl 39:5043–5051. https://doi.org/10.1016/j.eswa.2011.11.036

Pandey CK, Katiyar AK (2013) Solar Radiation: Models and Measurement Techniques. J Energy 2013:1–8. https://doi.org/10.1155/2013/305207

Park I, Kim HS, Lee J et al (2019) Temperature prediction using the missing data refinement model based on a long short-term memory neural network. Atmosphere (basel) 10:1–16. https://doi.org/10.3390/atmos10110718

Piri J, Kisi O (2015) Modelling solar radiation reached to the Earth using ANFIS, NN-ARX, and empirical models (Case studies: Zahedan and Bojnurd stations). J Atmos Solar-Terrestrial Phys 123:39–47. https://doi.org/10.1016/j.jastp.2014.12.006

Qing X, Niu Y (2018) Hourly day-ahead solar irradiance prediction using weather forecasts by LSTM. Energy 148:461–468. https://doi.org/10.1016/j.energy.2018.01.177

Şenocak F (2018) Forecasting of weighted average electricity market clearing price using artificial neural networks and anfis. Karadeniz Teknik Üniversitesi

Shamim MA, Bray M, Remesan R, Han D (2015) A hybrid modelling approach for assessing solar radiation. Theor Appl Climatol 122:403–420. https://doi.org/10.1007/s00704-014-1301-1

Sharifi SS, Rezaverdinejad V, Nourani V, Behmanesh J (2022) Multi-time-step ahead daily global solar radiation forecasting: performance evaluation of wavelet-based artificial neural network model. Meteorol Atmos Phys 134:1–14. https://doi.org/10.1007/s00703-022-00882-w

Sorkun MC, Durmaz Incel Ö, Paoli C (2020) Time series forecasting on multivariate solar radiation data using deep learning (LSTM). Turkish J Electr Eng Comput Sci 28:211–223. https://doi.org/10.3906/elk-1907-218

Sözen A, Arcaklioglu E, Özalp M (2004) Estimation of solar potential in Turkey by artificial neural networks using meteorological and geographical data. Energy Convers Manag 45:3033–3052. https://doi.org/10.1016/j.enconman.2003.12.020

Sthitapragyan M, Patra PK, Sahoo SS (2015) Comparison and prediction of monthly average solar radiation data using soft computing approach for eastern India. Comput Intell Data Min. https://doi.org/10.1007/978-81-322-2202-6_28

Suyono H, Hasanah RN, Setyawan RA et al (2018) Comparison of solar radiation intensity forecasting using ANFIS and multiple linear regression methods. Bull Electr Eng Informatics 7:191–198. https://doi.org/10.11591/eei.v7i2.1178

Tao H, Ewees AA, Al-Sulttani AO et al (2021) Global solar radiation prediction over North Dakota using air temperature: Development of novel hybrid intelligence model. Energy Rep 7:136–157. https://doi.org/10.1016/j.egyr.2020.11.033

Temur A (2019) Comparison of ARIMA, LSTM and Hybrid Models in Establishing Sales Budgets: A Case of Production Facility. Sakarya University

Turan E (2018) Calculation of Surface Leakage Current by ANFIS in High Voltage Insulator

Wang L, Kisi O, Zounemat-Kermani M et al (2017) Prediction of solar radiation in China using different adaptive neuro-fuzzy methods and M5 model tree. Int J Climatol 37:1141–1155. https://doi.org/10.1002/joc.4762

Wu Y, Wang J (2016) A novel hybrid model based on artificial neural networks for solar radiation prediction. Renew Energy 89:268–284. https://doi.org/10.1016/j.renene.2015.11.070

Xiao Y, Yin Y (2019) Hybrid LSTM neural network for short-term traffic flow prediction. Inf. https://doi.org/10.3390/info10030105

Yin J, Deng Z, Ines AVM et al (2020) Forecast of short-term daily reference evapotranspiration under limited meteorological variables using a hybrid bi-directional long short-term memory model (Bi-LSTM). Agric Water Manag 242:106386. https://doi.org/10.1016/j.agwat.2020.106386

Zhang CJ, Wang HY, Zeng J et al (2020) Tiny-RainNet: a deep convolutional neural network with bi-directional long short-term memory model for short-term rainfall prediction. Meteorol Appl 27:1–11. https://doi.org/10.1002/met.1956

Zhou Y, Liu Y, Wang D et al (2021) A review on global solar radiation prediction with machine learning models in a comprehensive perspective. Energy Convers Manag 235:113960. https://doi.org/10.1016/j.enconman.2021.113960

Publisher's Note Springer Nature remains neutral with regard to jurisdictional claims in published maps and institutional affiliations.

Springer Nature or its licensor (e.g. a society or other partner) holds exclusive rights to this article under a publishing agreement with the author(s) or other rightsholder(s); author self-archiving of the accepted manuscript version of this article is solely governed by the terms of such publishing agreement and applicable law.